Defect stability in thorium monocarbide: An *ab initio* study*

Wang Chang-Ying(王昌英)[a)b)], Han Han(韩 晗)[a)c)], Shao Kuan(邵 宽)[a)b)], Cheng Cheng(程 诚)[a)c)†], and Huai Ping(怀 平)[a)c)‡]

[a)] *Shanghai Institute of Applied Physics, Chinese Academy of Sciences, Shanghai* 201800, *China*
[b)] *University of Chinese Academy of Sciences, Chinese Academy of Sciences, Beijing* 100049, *China*
[c)] *Key Laboratory of Nuclear Radiation and Nuclear Energy Technology, Chinese Academy of Sciences, Shanghai* 201800, *China*

(Received 6 January 2015; revised manuscript received 3 April 2015; published online 21 July 2015)

The elastic properties and point defects of thorium monocarbide (ThC) have been studied by means of density functional theory based on the projector-augmented-wave method. The calculated electronic and elastic properties of ThC are in good agreement with experimental data and previous theoretical results. Five types of point defects have been considered in our study, including the vacancy defect, interstitial defect, antisite defect, schottky defect, and composition-conserving defect. Among these defects, the carbon vacancy defect has the lowest formation energy of 0.29 eV. The second most stable defect (0.49 eV) is one of composition-conserving defects in which one carbon is removed to another carbon site forming a C_2 dimer. In addition, we also discuss several kinds of carbon interstitial defects, and predict that the carbon trimer configuration may be a transition state for a carbon dimer diffusion in ThC.

Keywords: thorium monocarbide, *ab initio* study, bulk properties, defects

PACS: 71.15.Mb, 71.20.−b, 61.72.J−, 61.72.jj **DOI:** 10.1088/1674-1056/24/9/097101

1. Introduction

Actinide carbides are considered to be one of the most promising nuclear fuel materials of generation-IV reactors. They have several advantages relative to standard actinide oxide fuels,[1–3] such as a higher density, a higher thermal conductivity, and a better compatibility with clad materials.[4,5] The relevant studies were concerned with both technological developments and fundamental scientific aspects. Previously, researchers have widely studied uranium carbide[6–12] and mixed uranium-plutonium carbide.[13,14] From the 1960s to 1970s, as a supplement for fertile fuel, thorium-based nuclear power was recognized and built as an experimental reactor by the Oak Ridge National Laboratory. Afterwards, thorium carbide and uranium carbide fuel were designed and developed in the peach bottom reactor project.[15] After several decades' intermission, the relevant experimental and theoretical studies for thorium carbide are attracting a great deal of attention.

Experimentally, thorium monocarbide (ThC) has a large domain of nonstoichiometry (ThC_x with $0.55 < x < 1$ at high temperature).[16] There are several relevant experimental works on thorium carbide which were mainly reported in the 1960s and 1980s.[17–21] Through the investigation of the non-stoichiometry of ThC by Satow,[18] it can be deduced that the lattice defects of this compound are carbon vacancies. Gerward *et al.* did not observe structural phase transformation of ThC over the whole pressure range through the high-pressure x-ray diffraction studies.[16]

Theoretically, a few first-principle studies have been performed to understand the structural, electronic, elastic, and thermodynamic properties of ThC.[22–29] Shein *et al.* calculated the electronic, structural, and mechanical properties of ThC from the first-principles study.[22–25] Das *et al.* studied the electronic structure and elastic properties of transition metal series (Sc, Ti, V, Zr, and Hf) and actinides (Th, U) carbide based on the tight-binding linear muffin-tin orbitals method, and they found that the f states have features rather different from transition metal carbides.[26] Lim *et al.* studied the electronic properties of ThC by using Gaussian-type orbitals and density functional theory, and they found that Heyd–Scuseria–Ernzerhof (HSE) hybrid functional does not open a band gap near the Fermi energy in ThC.[27] Aydin *et al.* studied the pressure dependency of the structural, elastic and mechanical properties by using a first-principle method based on the LDA+U functional.[28] Pérez *et al.* reported the phonon and thermodynamic properties of ThC based on the density functional perturbation theory and harmonic approximation.[29]

It is well known that defects are unavoidable in nuclear fuel due to the irradiation damage from high-energy neutrons. However, there are few theoretical works about the defect of ThC. Based on the experimental observations, Matzke[30] wrote a review about the defects for ThC, and he speculated two important points: (i) there are important atomic displace-

*Project supported by the International S&T Cooperation Program of China (Grant No. 2014DFG60230), the National Natural Science Foundation of China (Grant No. 91326105), the National Basic Research Program of China (Grant No. 2010CB934504), and the Strategic Priority Research Program of the Chinese Academy of Sciences (Grant No. XDA02040104).

†Corresponding author. E-mail: chengcheng@sinap.ac.cn
‡Corresponding author. E-mail: huaiping@sinap.ac.cn

© 2015 Chinese Physical Society and IOP Publishing Ltd

ments around carbon vacancies; (ii) there is no indication of antistructure defects in ThC. In our following study, the two conclusions will be verified by us.

Our paper is organized as follows. In Section 2, the calculation details will be described. In Section 3, the calculated results will be presented and discussed. In Section 4, the conclusion remarks will be presented.

2. Calculation methods

All of these calculations were performed within the framework of density functional theory (DFT) and more particularly with the *ab initio* method[31,32] as implemented in the Vienna *ab initio* simulation package (VASP) code.[33] The generalized gradient approximation (GGA) to the exchange-correlation interaction was used.[34] Twelve electrons ($6s^26p^65f^06d^27s^2$) for thorium and four electrons ($2s^22p^2$) for carbon were taken into account as valence electrons. An energy cut-off of 500 eV for the plane-wave expansion of the electron basis was used. The convergence criteria have been chosen to be 10^{-6} eV, and 10^{-2} eV/Å for the total energy, and for the forces, respectively. When computing the total energy of a defected structure, the lattice constants were fixed, while the atomic coordinates were allowed to relax. The Brillouin zone is sampled by a $4\times4\times4$ Monkhorst–Pack k-point mesh[35] for a 64-atoms supercell. The bulk properties of ThC were calculated in a conventional cell which contains four carbon atoms and four thorium atoms with a $16\times16\times16$ k-point grid being used to sample the Brillouin zone. The calculation of electronic density of states (DOS) and electronic band structure were in a more rigorous condition with an energy cut-off of 600 eV and a $20\times20\times20$ k-point grid in a conventional cell.

3. Results and discussion

3.1. Bulk properties of ThC

The bulk properties of ThC including the lattice parameters, the bulk modulus, and the electronic properties were calculated from the *ab initio* method, and compared with the previous theoretical and experimental results. As a whole, the current method with the GGA describes these properties pretty well.

In detail, thorium monocarbide (ThC) has a face-centered cubic lattice as shown in Fig. 1. Our calculated lattice parameter and bulk modulus obtained from the GGA are 5.352 Å and 133.33 GPa, which agree well with the experimental values of 5.335 Å and 125 GPa, respectively. However, the calculated results from the LDA do not fit well with the experiment as shown in Table 1, in particular for the bulk modulus with a relatively large error of 15.9%. Our results demonstrate that the GGA is much better than the LDA. Therefore, the GGA functional is adopted in the rest of this work.

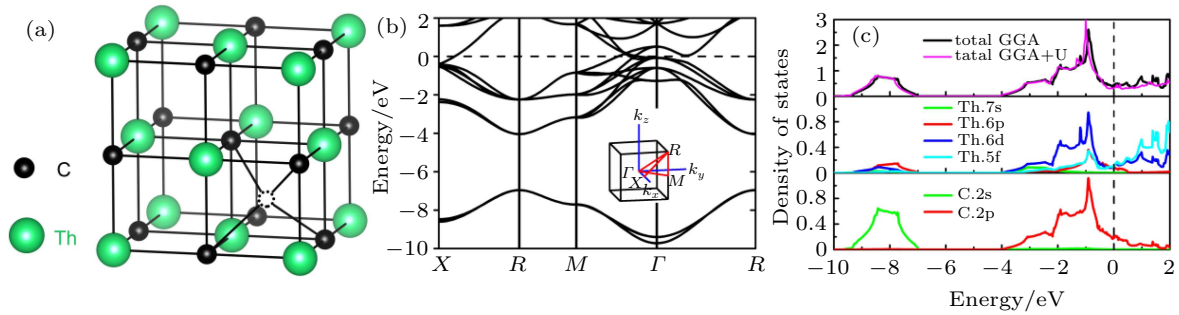


Fig. 1. (color online) (a) Crystal structure of ThC. Black dotted circle represents tetrahedral interstitial site. (b) Electronic band structure and (c) total density of state as well as projected density of states of ThC.

The electronic band structure and total DOS as well as projected DOS calculated by GGA are shown in Figs. 1(b) and 1(c), respectively. The total DOS is also calculated by using GGA + U ($U_{\rm eff}=4$ eV), as shown in Fig. 1(c). The profiles of total DOS for these two kinds of methods are almost the same. It means that for the ThC system the strong correlation effect of f orbital electrons can be ignored and the electronic properties can be described sufficiently by using the GGA method. Both Figs. 1(b) and 1(c) show that there is no band gap between the valence and conduction band, indicating that ThC is metal. The electrons around the Fermi level come mainly from Th-5f, Th-6d, and C-2p states, which are mostly located around the Γ point. The conduction band is strongly dominated by Th 5f and Th 6d states, with a little bit of the degree of C 2p states. As for the valence band, the hybridization of C 2p states with the Th 6d states from -4 eV up to the Fermi energy level contributes to Th-C interaction. Our calculated electronic properties agree well with the previous theoretical results by Aydin *et al.*[28] Our Bader charge density analysis provides 1.84 electrons charge transfer from Th atom to C atom, with respect to their original electron occupation. In the previous calculation of uranium monocarbide UC,[8] a Bader charge transfer of 1.6 electrons occurs from U atom to C atom. The relatively larger charge transfer value of ThC reflects that the carbon atom takes more electrons away

from thorium than uranium.

Table 1. Calculated equilibrium lattice parameters a and bulk modulus B of ThC. Δa and ΔB are the relative errors of calculated results compared with the experimental values.

	a/Å	B/GPa	Δa/%	ΔB/%
Exp.	5.335 – 5.344[a]	125[b]		
LDA	5.268 (5.269[c])	144.83 (143.41[c])	−1.339	15.9
GGA	5.352 (5.341[c])	133.33 (134.33[c])	0.234	6.7

[a]Experimental value in Ref. [16]

[b]Experimental value in Ref. [36]

[c]Theoretical results in Ref. [28]

3.2. Single point defects and complex defects

We mainly study five types of point defects including vacancy defect, interstitial defect, antisite defect, schottky defect, and composition-conserving defect. To calculate the defect formation energy of single point defects, we use the following formula for one vacancy (V_X) or one interstitial defect (I_X) (where X labels thorium or carbon defect). The formation energies $E^{\mathrm{F}}_{V_X,I_X}$ are

$$E^{\mathrm{F}}_{V_X,I_X} = E_{V_X,I_X} - E^{\mathrm{N}} \pm E_x, \tag{1}$$

where E^{N} is the energy of the defect-free ThC supercell, E_{V_X,I_X} is the energy of the supercell containing corresponding defects, and E_x is the energy per atom of each chemical species in its reference state. Here the reference states are the ground-state crystalline phases of thorium and carbon, namely, the α-thorium crystal and the carbon graphite phase.

As we know that a point defect would interact with its image in the adjacent supercell because of the periodic boundary conditions in our calculation method. Therefore, five different supercell sizes were tested to check the convergence of the formation energy including $1\times1\times1$ (8 atoms), $2\times1\times1$ (16 atoms), $2\times2\times1$ (32 atoms), $2\times2\times2$ (64 atoms), and $3\times2\times2$ (96 atoms). Two types of interstitial defects including Th tetrahedral interstitial defect (I_{Th}) and C_2 dimer defect along the $\langle110\rangle$ direction were chosen to justify the convergence as illustrated in Table 2. The table shows that the difference in the formation energy for the I_{Th} between a 64-atom and a 96-atom supercell is 0.117 eV. Therefore, we conclude that the calculated formation energies are well converged in a 64-atoms supercell. Eventually, the 64-atoms supercell will be taken in our remaining calculations.

Table 2. Formation energies (eV) of Th tetrahedral interstitial defect (I_{Th}) and C_2 dimer defect along the $\langle110\rangle$ direction in ThC as a function of the supercell sizes used in the calculation.

Supercells	$1\times1\times1$	$2\times1\times1$	$2\times2\times1$	$2\times2\times2$	$3\times2\times2$
I_{Th}	7.381	5.757	4.552	4.395	4.278
$C_2\langle110\rangle$	2.327	1.308	1.155	1.044	0.997

Concerning the single point defects, four types of defects will be considered in our study including single carbon vacancy (V_{C}), single thorium vacancy (V_{Th}), single carbon tetrahedral interstitial (I_{C}) defect, and single thorium tetrahedral interstitial defect (I_{Th}). The tetrahedral site is illustrated in Fig. 1(a), and the calculated formation energies for these defects are listed in Table 3. The table shows that among these defects the carbon vacancy has the lowest formation energy (0.29 eV). This is consistent with the experimental observations,[18,37] in which the carbon vacancies were considered to be the predominant defects in the nonstoichiometric ThC. It is noted that our result for the carbon vacancy is also in good agreement with the previous result (0.32 eV) by Shein *et al.*,[24] in which this energy was calculated by the full-potential DFT in an eight-atom supercell. The calculated energy for the tetrahedral interstitial carbon (I_{C}) is quite high (3.67 eV), indicating that this kind of defect is almost impossible in ThC. According to Table 3, the carbon vacancy and carbon interstitial defects have lower formation energies than the thorium vacancy and thorium interstitial defects, respectively. This phenomenon is consistent with that in UC,[8] in which the radiation damage and deviation from stoichiometry are more probably generated in the carbon sublattice.

Table 3. Formation energies (E_{form}) of carbon/thorium vacancy (V_{C} and V_{Th}) and tetrahedral interstitial (I_{Th} and I_{C}) defects, as well as atomic displacements of the first shell (s) and second shell (s) (δR) due to the presence of point defects in ThC. Negative (positive) value indicates a decrease (increase) of the interatomic distance with relating element symbol in parentheses.

	E_{form}/eV	$\delta R_{\mathrm{first}}$/Å	$\delta R_{\mathrm{second}}$/Å
V_{Th}	5.75	+0.276(C)	−0.046(Th)
V_{C}	0.29	+0.088(Th)	−0.023(C)
V_{C}	0.32[24]		
I_{Th}	4.39	+0.531(Th)/+0.088(C)	+0.022(Th)/+0.132(C)
I_{C}	3.67	+0.187(Th)/−0.487(C)	+0.012(Th)/+0.091(C)

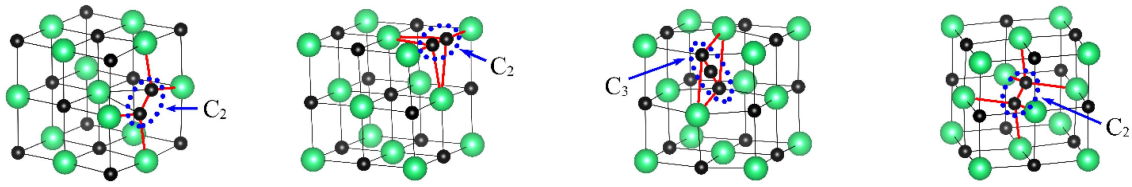
As we know that due to the defects the atomic position will deviate from the original (equilibrium) one. This deviation is defined as the atomic displacements δR, i.e., changes in atomic separation distance due to the presence of the defect. The displacements for the above four defects were calculated and presented in Table 3. For the single carbon vacancy defect, Table 3 shows that the displacements of the first nearest neighbor (1NN) thorium atoms are in the order of 0.088 Å. This is consistent with the experimental results of ThC_{1-x} obtained by neutron diffraction,[38] which indicates that the displacements of neighboring Th atoms are in the order of $\approx 2\%$ of the lattice parameter. For the thorium vacancy defect, the displacements of the 1NN atoms of 0.276 Å are induced. For the carbon tetrahedral interstitial defect, Table 3 shows that this causes the inward displacements of carbon atoms of 0.487 Å, and conversely this causes the outwards displacements of the thorium atoms of 0.187 Å. Concerning the thorium tetrahedral interstitial defect, it induces the largest perturbation on its surrounding atoms as shown in Table 3, i.e., the thorium

and carbon atoms move outward of 0.531 Å and 0.088 Å, respectively. Actually, this defect also has the largest effect on the second near neighboring (2NN) atoms among the four defects, i.e., the displacements for the defect is 0.132 Å, and the displacements for the other three defects are almost zero.

Concerning the complex interstitial defects, we have studied the stabilities of C_3 trimer and C_2 dimers along different crystallographic orientations as sketched in Fig. 2. Their formation energies are listed in Table 4. The table shows that the C_2 dimer along the $\langle 110 \rangle$ direction has the lowest formation energy of 1.04 eV among these defects. This rationalizes the experimental conclusion that some introduced carbon atoms could link with the existing carbon atoms to form "C_2" groups as high carbon compositions are reached in ThC.[39] It is noted that the energy differences among these defects are small with the largest one being 0.22 eV, suggesting that they could possibly coexist in ThC. Considering the similar energy level between the dimer and the trimer according to Table 4, we can predict that the C_3 trimer configuration may be a transition state of the C_2 dimer diffusion in ThC. We also present the charge density map of the dimer and the trimer in Fig. 3. The figure shows that it is the carbon–carbon bonding interaction that stabilizes these defects.

Table 4. Formation energies of complex defects, including C_2 dimer ($C_2\langle 110 \rangle$, $C_2\langle 100 \rangle$, and $C_2\langle 111 \rangle$), C_3 trimer (C_2), antisite defects (C_{Th} and Th_C), Frenkel carbon (FP_C), Frenkel thorium (FP_{Th}), Schottky (Sch), $C_2\langle 100 \rangle$ dimer plus carbon vacancy ($C_2\langle 100 \rangle + V_C$), and trimer C_3 plus carbon vacancy defects ($C_3 + V_C$).

	$C_2\langle 110 \rangle$	$C_2\langle 100 \rangle$	C_3	$C_2\langle 111 \rangle$
Interstitial defects	1.04	1.13	1.16	1.26
	C_{Th}	Th_C		
Antisite defects	10.47	5.72		
	Sch			
Schottky defects	4.79			
	FP_C	FP_{Th}	$C_2\langle 100 \rangle + V_C$	$C_3 + V_C$
Composition-conserving defects	3.96	10.14	0.49	1.25



(a) $d(\mathrm{C-C}) = 1.309$ Å (b) $d(\mathrm{C-C}) = 1.314$ Å (c) $d(\mathrm{C-C}) = 1.375$ Å (d) $d(\mathrm{C-C}) = 1.299$ Å

Fig. 2. View of (a) $C_2\langle 110 \rangle$, (b) $\langle 100 \rangle$, and (d) $\langle 111 \rangle$ dimer together with (c) C_3 trimer. Th atoms in green, C atoms in black. d (C–C) represents the C–C distance of C_2 dimer and C_3 trimer.

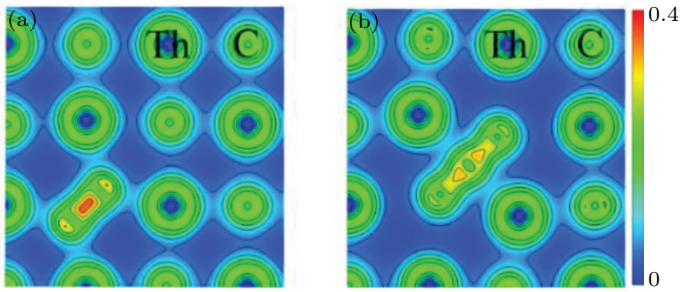


Fig. 3. Charge density distribution graph in (010) plane of ThC for (a) $C_2\langle 110 \rangle$ dimer and (b) C_3 trimer. Red color for high electron density and blue color for low electron density. The contour interval is 0.05 electrons/Bohr^3.

To calculate the defect formation energy of the complex defects, we use the following formulas. For an antisite defect (removing a B atom from its current position and replacing it by an A atom), formation energy $E^{\mathrm{F}}_{A_{\mathrm{B}}}$ reads

$$E^{\mathrm{F}}_{A_{\mathrm{B}}} = E_{A_B} - E^{\mathrm{N}} - E_{\mathrm{A}} + E_{\mathrm{B}}. \quad (2)$$

For a bound Frenkel pair, the formation energy $E^{\mathrm{F}}_{\mathrm{FP}_X}$ reads

$$E^{\mathrm{F}}_{\mathrm{FP}_X} = E_{\mathrm{FP}_X} - E^{\mathrm{N}}. \quad (3)$$

For a bivacancy, the formation energy $E^{\mathrm{F}}_{\mathrm{BiVac}_{XX'}}$ reads

$$E^{\mathrm{F}}_{\mathrm{BiVac}_{XX'}} = E_{\mathrm{BiVac}_{XX'}} - E^{\mathrm{N}} + E_x + E_{x'}, \quad (4)$$

where E^{N} is the energy of the defect-free ThC supercell, $E_{A_{\mathrm{B}}}$, E_{FP_X}, and $E_{\mathrm{BiVac}_{XX'}}$ are the energies of the supercell containing corresponding defects, E_x, E_{A}, and E_{B} are the energy per atom of each chemical species in its reference state. Here the reference states are the ground-state crystalline phases of thorium and carbon, namely, the α-thorium crystal and the carbon graphite phase.

The antisite defect is an exchange of one Th and one C atom in ThC. The calculated formation energies of carbon antisite and thorium antisite are listed in Table 4. The table shows that the energies for the two defects are quite high

(larger than 5 eV), indicating that the two defects are unstable. This is in line with the experimental observation, in which the antisite defects were not observed in ThC.[27]

The Schottky defect is a type of electrical neutrality point defect in which an equal number of cations and anions are missing from their lattice sites and the stoichiometry of the crystal is maintained. In ThC, the Schottky defects are resulted from the simultaneous creation of thorium and carbon vacancies as illustrated in Fig. 4. The calculated formation energy for this defect is 4.79 eV as listed in Table 4. This value is lower by about 1.25 eV than the sum of the energies of the isolated thorium and carbon vacancy defects (as listed in Table 3). This phenomenon suggests that the defect will be stabilized when thorium and carbon vacancies are placed as the first neighbor. It is in accordance with the properties of a Schottky defect for UC.[8,9] Therefore, the widely existing carbon vacancy may aggregate together around the thorium vacancy in ThC.

Since single point defects alone are not composition-conserving, then thermal defects have to appear in balanced combinations in order to maintain the overall composition of ThC crystal. Actually at finite temperature, thermal defects will be activated in ThC. Usually the composition-conserving defects are in pairs of single point defects or in more complex forms.

The most common composition-conserving defect is a Frenkel pair. There are two kinds of common Frenkel defects: one is the carbon Frenkel pair as illustrated in Fig. 5(a), and another is the thorium Frenkel pair as illustrated in Fig. 5(b). The calculated formation energies for the two defects are listed in Table 4. It shows that the energies for the two cases (3.96 eV and 10.14 eV, respectively) are quite high, indicating that the two defects may not exist.

In addition, we have also considered two special types of Frenkel defects: one is a carbon dimer plus a carbon vacancy as indicated in Fig. 5(c), and another is a carbon trimer plus a carbon vacancy as indicated in Fig. 5(d). The formation energies for the two defects are presented in Table 4. Interestingly, the energy for the carbon dimer plus carbon vacancy is as low as 0.49 eV. This value is close to that (0.29 eV) for a single carbon vacancy, indicating that this kind of defect could be stable. This is consistent with the literature view which states that ThC may contain some C_2 groups compensated by some carbon vacancies.[40] The energy for the carbon trimer plus carbon vacancy is 1.25 eV which is a little higher than that of the carbon trimer (1.16 eV). The clustering of carbon vacancy and carbon trimer is also favored from the energy point of view at high temperature. In consideration of the existence of the C_2 dimer plus the carbon vacancy discussed above, the C_3 trimer plus vacancy might be a transition state of the C_2 dimer diffusion in ThC.

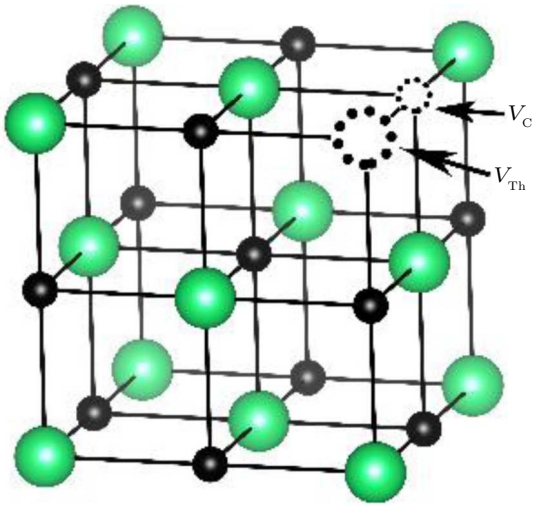


Fig. 4. (color online) The diagram for Schottky defect: the positions of carbon vacancy (V_C) and of thorium vacancy (V_{Th}) are indicated by the arrows. Th atoms in green, C atoms in black, carbon vacancy and thorium vacancy in black dotted circle.

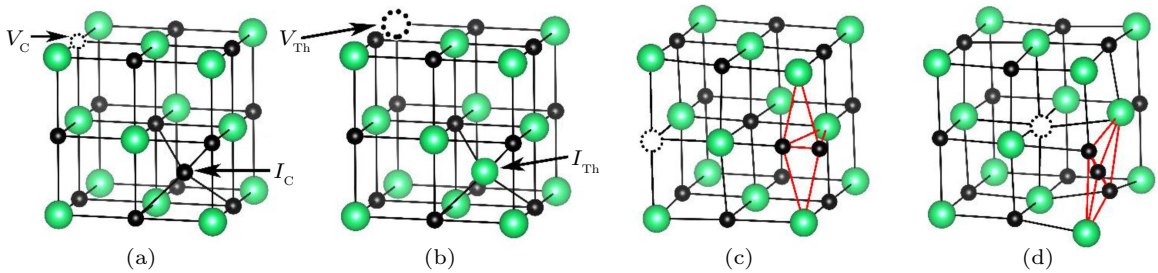


Fig. 5. (color online) (a) Simplified diagram for carbon Frenkel defect: the positions of the carbon vacancy (V_C) and of the carbon interstitial (I_C) are indicated by the arrows. (b) Simplified diagram for thorium Frenkel defect: the positions of the thorium vacancy (V_{Th}) and of the thorium interstitial (I_{Th}) are indicated by the arrows. (c) Carbon dimer plus carbon vacancy: a carbon vacancy (V_C) is formed and a carbon dimer (C_2) appears. (d) Carbon trimer plus carbon vacancy: a carbon vacancy (V_C) is formed and a carbon trimer (C_3) appears. Th atoms in green, C atoms in black, carbon vacancy and thorium vacancy in black dotted circle.

4. Conclusions

The defects of thorium monocarbide (ThC) have been studied by means of density functional theory based on the projector-augmented-wave method. Five types of point defects have been considered in our study including the vacancy defect, interstitial defect, antisite defect, schottky de-

fect and composition-conserving defect. Among these defects, the carbon vacancy defect has the lowest formation energy of 0.29 eV. This conclusion is consistent with the experimental phenomenon that the carbon vacancies are the predominant defects in nonstoichiometric ThC. Through the investigation of displacements (δR) for the single point defects, we have confirmed one experimental speculation that there are important atomic displacements around carbon vacancies. The second most stable defect (0.49 eV) is one of composition-conserving defects in which one carbon is removed to another carbon site forming a C_2 dimer (C_2 along the $\langle 100 \rangle$ direction). According to our calculations, we think that the C_3 trimer configuration may be a transition state of the C_2 dimer diffusion in ThC. Concerning the antistructure defects, our calculations have verified another experimental speculation that there is no antistructure defect in ThC.

References

[1] Li Q, Yang J S, Huang D H, Cao Q L and Wang F H 2014 *Chin. Phys. B* **23** 017101
[2] Li P, Jia T T, Gao T and Li G 2012 *Chin. Phys. B* **21** 043301
[3] Li L, Wang B T and Zhang P 2015 *Chin. Phys. Lett.* **32** 037102
[4] Sengupta A K, Agarwal R and Kamath S H 2012 in Comprehensive Nuclear Materials (ed. R. J. M. Konings) (Oxford: Elsevier) p. 55
[5] Lee W E, Gilbert M, Murphy S T and Grime R W 2013 *J. Am. Ceram. Soc.* **96** 2005
[6] Shi H, Zhang P, Li S S, Sun B and Wang B 2009 *Phys. Lett. A* **373** 3577
[7] Shi H, Zhang P, Li S S, Wang B and Sun B 2010 *J. Nucl. Mater.* **396** 218
[8] Freyss M 2010 *Phys. Rev. B* **81** 014101
[9] Ducher R, Dubourg R, Barrachin M and Pasturel A 2011 *Phys. Rev. B* **83** 104107
[10] Sahoo B D, Joshi K D and Gupta S C 2013 *J. Nucl. Mater.* **437** 81
[11] Carvajal Nuñez U, Martel U L, Prieur D, Lopez Honorato E, Eloirdi R, Farnan I, Vitova T and Somers J 2013 *Inorg. Chem.* **52** 11669
[12] Berthinier C, Rado C, Dugne O, Cabie M, Chatillon C, Boichot R and Blanquet E 2013 *J. Nucl. Mater.* **432** 505
[13] Petti D, Crawford D C and Chauvin N 2009 *MRS Bulletin* **34** 40
[14] Crawford D C, Porter D L and Hayes S L 2007 *J. Nucl. Mater.* **371** 202
[15] Everett III J L and Kohler E J 1978 *Ann. Nucl. Energy* **5** 321
[16] Kleykamp H 1992 *Thorium Carbides, Gmelin Handbook of Inorganic and Organometallic Chemistry*, Vol. C6 (Berlin: Springer)
[17] Kempter C P and Krikorian N H 1962 *J. Less Common Met.* **4** 244
[18] Satow T 1967 *J. Nucl. Mater.* **21** 255
[19] Gerward L, Olsen J S, Benedict U, Itie J P and Spirlet J C 1986 *J. Appl. Crystallogr.* **19** 308
[20] Yamawaki M, Koyama T and Takahashi Y 1989 *J. Nucl. Mater.* **167** 113
[21] Yamawaki M 1991 *Solid State Ionics* **49** 217
[22] Shein I R, Shein K I and Ivanovskii A L 2006 *J. Nucl. Mater.* **353** 19
[23] Shein I R, Shein K I, Shveikin G P and Ivanovskii A L 2006 *Dokl. Phys. Chem.* **407** 106
[24] Shein I R and Ivanovskii A L 2010 *Solid State Sci.* **12** 1580
[25] Shein I R and Ivanovskii A L 2010 *Phys. Solid State* **52** 2039
[26] Das T, Deb S and Mookerjee A 2005 *Physica B* **367** 6
[27] Lim I S and Scuseria G E 2008 *Chem. Phys. Lett.* **460** 137
[28] Aydin S, Tatar A and Ciftci Y O 2012 *J. Nucl. Mater.* **429** 55
[29] Pérez D, Jaroszewicz S, Llois A M and Mosca H O 2013 *J. Nucl. Mater.* **437** 135
[30] Matzke H 1984 *Solid State Ionics* **12** 25
[31] Blöchl P E 1994 *Phys. Rev. B* **50** 17953
[32] Kresse G and Joubert D 1999 *Phys. Rev. B* **59** 1758
[33] Kresse G and Furthmüller J 1996 *Phys. Rev. B* **54** 11169
[34] Perdew J P, Jackson K A, Pederson M R, Singh D J and Fiolhais C 1992 *Phys. Rev. B* **46** 6671
[35] Monkhorst H J and Pack J D 1976 *Phys. Rev. B* **13** 5188
[36] Benz R and Naoumidis A 1987 *Thorium Compounds with Nitrogen, Gmelin Handbook of Inorganic Chemistry*, Vol. C3 (Berlin: Springer)
[37] Lightstone J B and Libowitz G G 1969 *J. Phys. Chem. Solids* **30** 1025
[38] Moisy-Maurice V, de Novion C H and Convert P 1980 *Acta Crystallogr. A* **36** 916
[39] Murch G E and Thorn R J 1979 *J. Nucl. Mater.* **82** 430
[40] Manara D, De Bruycke F, Sengupta A K, Agarwal R and Kamath H S 2012 in *Comprehensive Nuclear Materials* (ed. J. M. K. Rudy) (Oxford: Elsevier), p. 87